Inventory of supplemental items D09-01745.

Figure S1. Suppression of NF1 leads to RA resistance in neuroblastoma cells independent of *MYCN* status. **Related to figure 1.**

Figure S2. NF1 loss down-regulates *ZNF423* in other neuroblastoma cells and ZNF423 expression and RA sensitivity in a panel of neuroblastoam cell lines. **Related to figure 4.**

Figure S3. Absence of NF1 protein expression is significantly associated with resistance to RA and lower levels of *ZNF423* in a panel of neuroblastoma cell lines. **Related to figure 6.**

Figure S4. Deletion analysis of the NF1 genomic locus in SJ-NB10 and SK-N-F1 cells by SNP microarrays and sequence analysis of the NF1 H553R missense mutation in a primary ganglioneuroma**. Related to figure 6.**

Figure S5. Induction of ZNF423 by MEK inhibitor treatment and hyperactivation of RARß in the combination with RA in SK-N-AS cells, a neuroblastoma cell line with naturally occurring low NF1**. Related to figure 7.**

Table S1. The list of genes regulated by knockdown of NF1 in SH-SY5Y cells. **Related to figure 4.**

Table S2. Multivariate analysis of the AMC and Oberthuer cohorts. **Related to figure 5.**

Supplemental Experimental Procedures

Supplemental References.

Fig S1

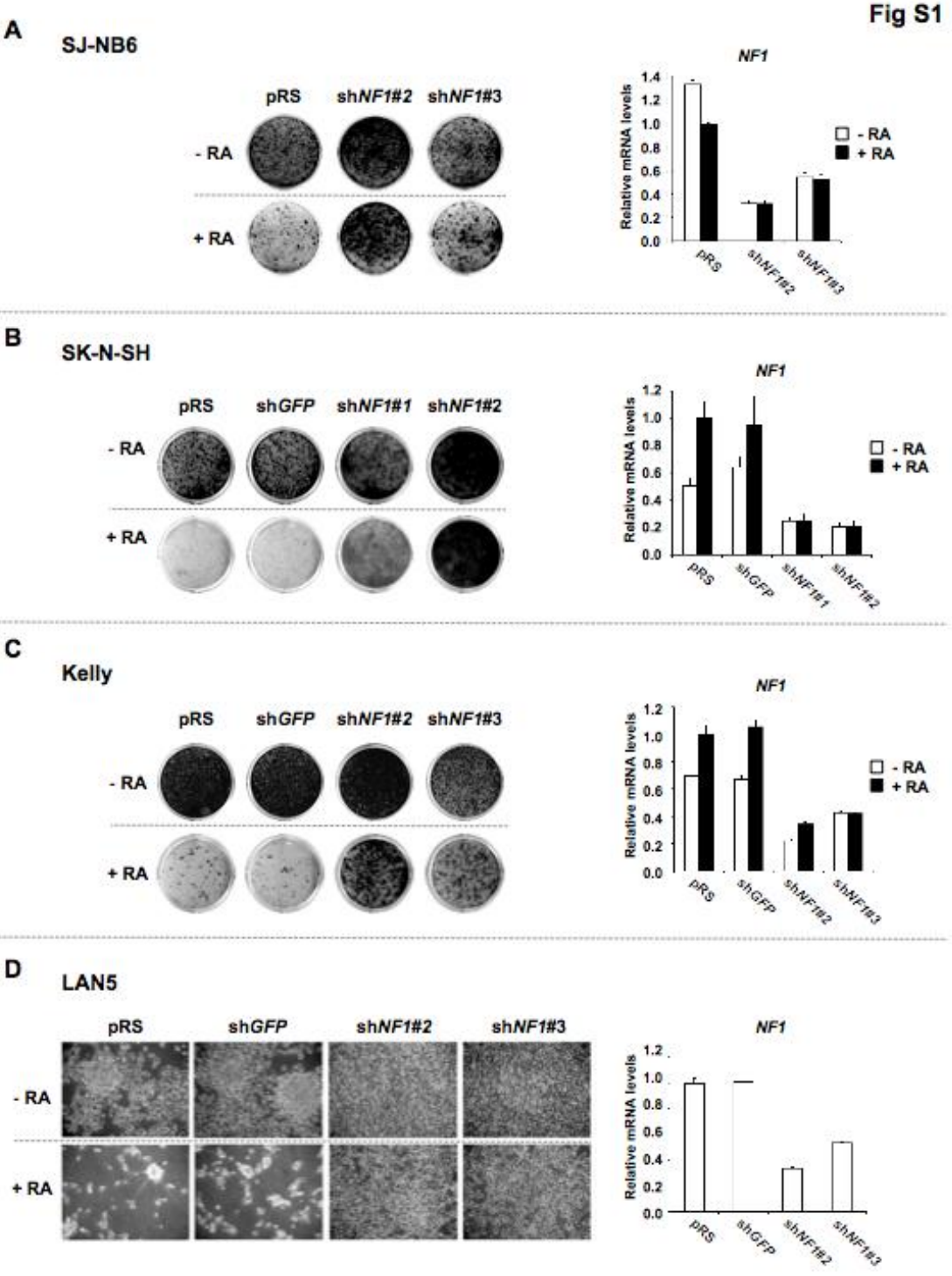
A
SJ-NB6
pRS
shNF1#2
shNF1#3
- RA
+ RA
NF1
Relative mRNA levels
1.4
1.2
1.0
0.8
0.6
0.4
0.2
0.0
- RA
+ RA
pRS
shNF1#2
shNF1#3
B
SK-N-SH
pRS
shGFP
shNF1#1
shNF1#2
- RA
+ RA
NF1
Relative mRNA levels
1.2
1.0
0.8
0.6
0.4
0.2
0.0
- RA
+ RA
pRS
shGFP
shNF1#1
shNF1#2
C
Kelly
pRS
shGFP
shNF1#2
shNF1#3
- RA
+ RA
NF1
Relative mRNA levels
1.2
1.0
0.8
0.6
0.4
0.2
0.0
- RA
+ RA
pRS
shGFP
shNF1#2
shNF1#3
D
LAN5
pRS
shGFP
shNF1#2
shNF1#3
- RA
+ RA
NF1
Relative mRNA levels
1.2
1.0
0.8
0.6
0.4
0.2
0.0
pRS
shGFP
shNF1#2
shNF1#3

Figure S1. Suppression of NF1 leads to RA resistance in neuroblastoma cells independent of *MYCN* status. Related to figure 1.

(A) SJ-NB6 cells (*MYCN* amplified) expressing controls or shRNAs targeting *NF1* were grown in the absence or presence of RA (100 nM). The cells were fixed, stained and photographed after 21 days (untreated) or 35 days (RA treatment). *NF1* mRNA levels were measured by qRT-PCR. Error bars denote SD.

(B) SK-N-SH cells (non-*MYCN* amplified) expressing controls or shRNAs targeting *NF1* were grown in the absence or presence of RA (100 nM). The cells were fixed, stained and photographed after 14 days (untreated) or 21 days (RA treatment). *NF1* mRNA levels were measured by qRT-PCR. Error bars denote SD.

(C) Kelly cells (*MYCN* amplified) expressing controls or shRNAs targeting *NF1* were grown in the absence or presence of RA (100 nM). The cells were fixed, stained and photographed after 14 days (untreated) or 21 days (RA treatment). *NF1* mRNA levels were measured by qRT-PCR. Error bars denote SD.

(D) LAN-5 cells (*MYCN* amplified) expressing controls or shRNAs targeting *NF1* were grown in the absence or presence of RA (100 nM). As the cells are poorly adhesive, they were not fixed and stained but instead photographed after 12 days. *NF1* mRNA levels were measured by qRT-PCR. Error bars denote SD.

Fig S2

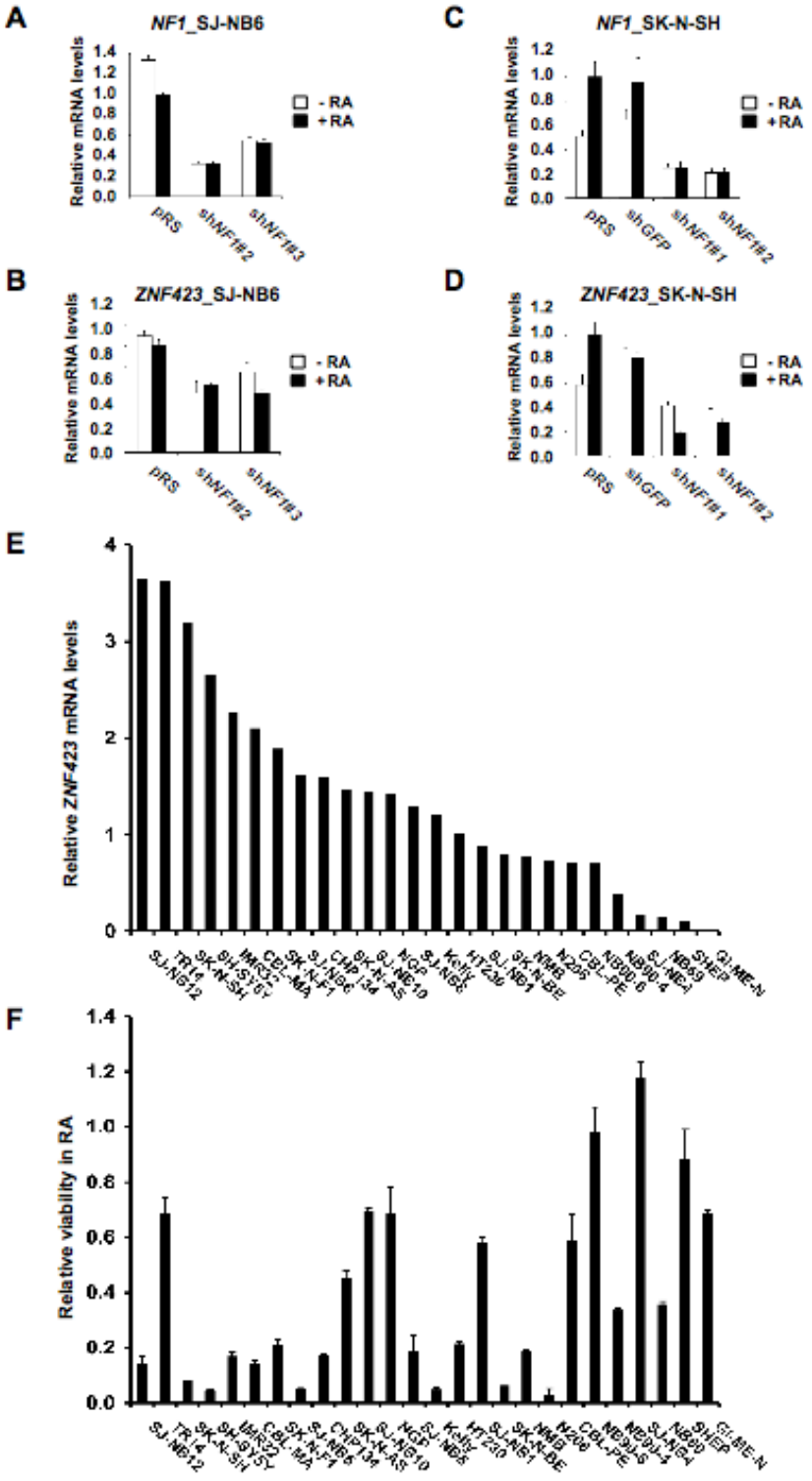
A
NF1_SJ-NB6
Relative mRNA levels
- RA
+ RA
pRS
shNF1#2
shNF1#3
C
NF1_SK-N-SH
shGFP
shNF1#1
shNF1#2
B
ZNF423_SJ-NB6
D
ZNF423_SK-N-SH
E
Relative ZNF423 mRNA levels
F
Relative viability in RA

Figure S2. NF1 loss down-regulates *ZNF423* in other neuroblastoma cells and ZNF423 expression and RA sensitivity in a panel of neuroblastoma cell lines. Related to figure 4.

NF1 knockdown leads to down-regulation of *ZNF423* in SJ-NB6 (A and B) and SK-N-SH (C and D) cells. Cells expressing controls and shRNAs targeting *NF1* were grown in the absence or presence of RA (100 nM) for 7 days and mRNA levels of the *NF1* (A and C) and *ZNF423* (B and D) were measured by qRT-PCR. Error bars denote SD.

(E) *ZNF42*3 mRNA levels in a panel of 26 different neuroblastoma cell lines were measured by qRT-PCR.

(F) RA sensitivity of 26 different neuroblastoma cell lines. The relative viability in 100nM RA was determined by the ratio of cell growth of treated versus untreated cultures measured by crystal violet quantification after long-term colony formation assays.

Fig S3

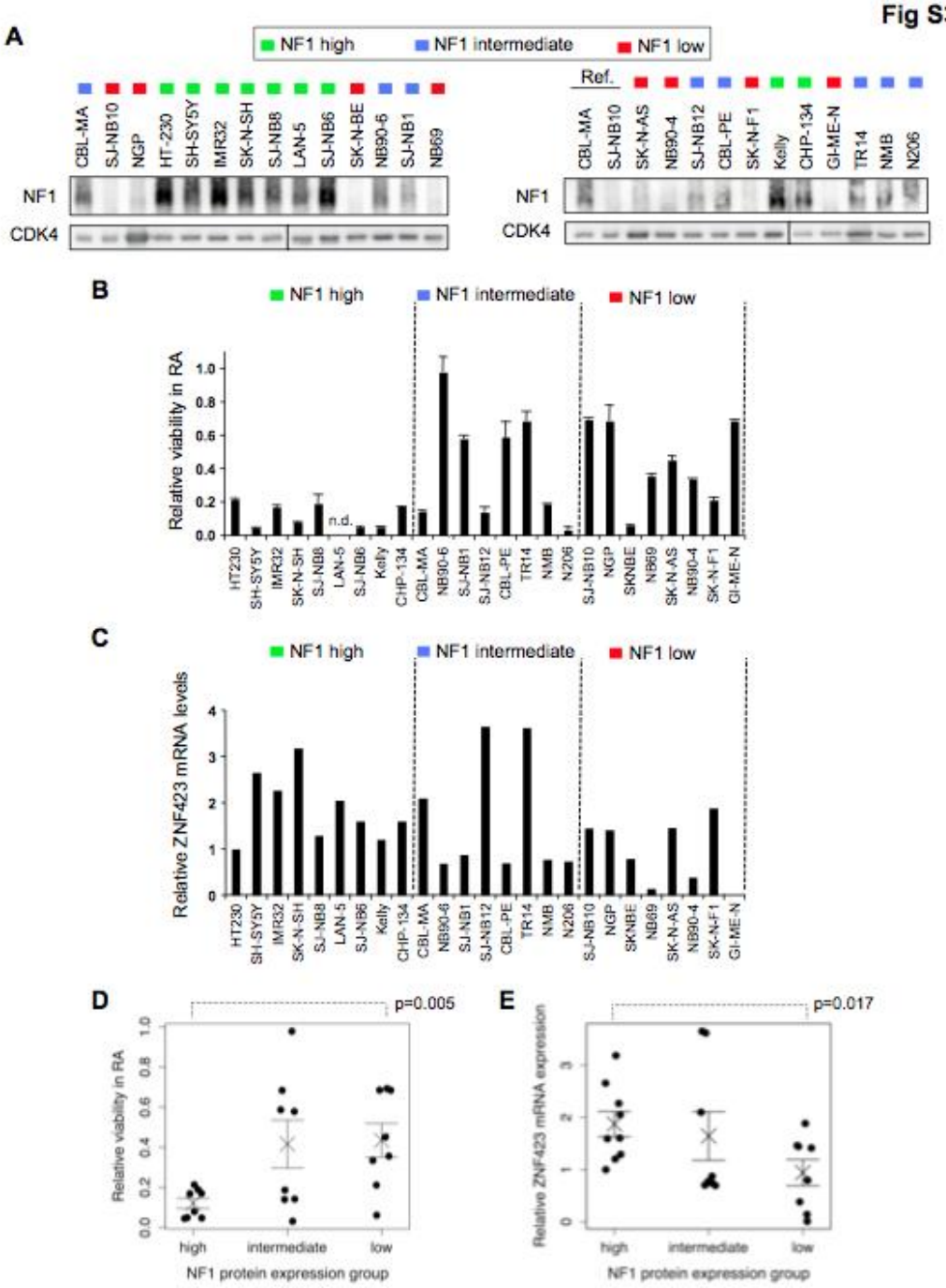
A
NF1 high
NF1 intermediate
NF1 low
CBL-MA
SJ-NB10
NGP
HT-230
SH-SY5Y
IMR32
SK-N-SH
SJ-NB8
LAN-5
SJ-NB6
SK-N-BE
NB90-6
SJ-NB1
NB69
Ref.
CBL-MA
SJ-NB10
SK-N-AS
NB90-4
SJ-NB12
CBL-PE
SK-N-F1
Kelly
CHP-134
GI-ME-N
TR14
NMB
N206
NF1
CDK4
B
NF1 high
NF1 intermediate
NF1 low
Relative viability in RA
n.d.
C
NF1 high
NF1 intermediate
NF1 low
Relative ZNF423 mRNA levels
D
p=0.005
Relative viability in RA
high
intermediate
low
NF1 protein expression group
E
p=0.017
Relative ZNF423 mRNA expression
high
intermediate
low
NF1 protein expression group

Figure S3. Absence of NF1 protein expression is significantly associated with resistance to RA and lower levels of *ZNF423* in a panel of neuroblastoma cell lines. Related to figure 6.

(A) NF1 protein levels were determined in a panel of neuroblastoma cell lines by Western blotting and grouped into high, intermediate and low (see also figure 6A). The cell lines CBL-MA (intermediate) and SJ-NB10 (low) served as references.

Relative viability in RA (B) and *ZNF423* (C) of the indicated neuroblastoma cell lines as grouped by NF1 protein expression levels. Relative *ZNF423* mRNA expression levels were determined by qRT-PCR. Relative viability in RA for LAN-5 was not determined (n.d.), as these cells are poorly adhesive and could not be properly fixed for crystal violet quantification. Nevertheless, LAN-5 is highly sensitive to RA as shown in figures S1D. LAN-5 was also excluded from the statistical analysis (see below).

(D) $NF1^{high}$ neuroblastoma cell lines are significantly more sensitive to RA than NF^{low} cells (p=0.005, Wilcoxon-test). Differences between the other subgroups were not significant. Crosses indicate mean values and error bars denote SEM.

(E) $NF1^{high}$ neuroblastoma cell lines express significantly higher levels of *ZNF423* than $NF1^{low}$ cells (p=0.017, t-test). Crosses indicate mean values and error bars denote SEM. Differences between the other subgroups were not significant.

Fig S4

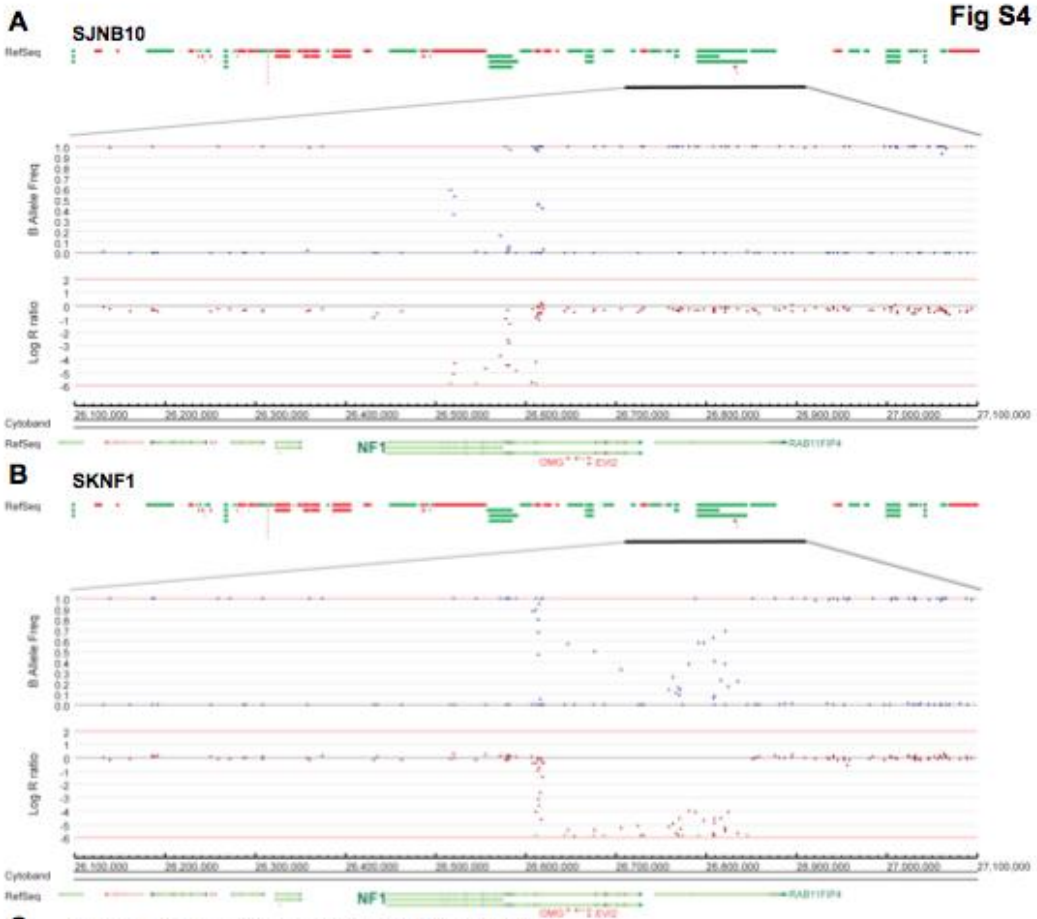
A
SJNB10
RefSeq
B Allele Freq
Log R ratio
Cytoband
RefSeq
NF1
RAB11FIP4
B
SKNF1
RefSeq
B Allele Freq
Log R ratio
Cytoband
RefSeq
NF1
RAB11FIP4

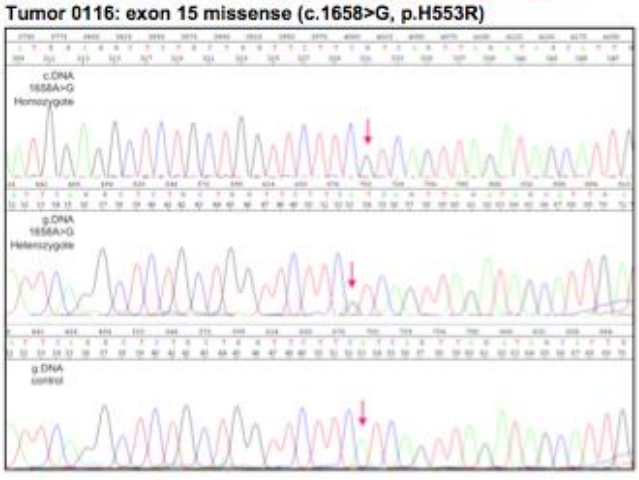
C
Tumor 0116: exon 15 missense (c.1658>G, p.H553R)
c.DNA
1658A>G
Homozygote
g.DNA
1658A>G
Heterozygote
g.DNA
control

Figure S4. Deletion analysis of the *NF1* genomic locus in SJ-NB10 and SK-N-F1 cells by SNP microarrays and sequence analysis of the NF1 H553R missense mutation in a primary ganglioneuroma. Related to figure 6.

The panel represents a close-up view of the genomic *NF1* locus of SJ-NB10 (A) and SK-N-F1 (B) neuroblastoma cells. B allele frequencies (B Allele Freq) and signal intensities (Log R ratio) are indicated. Homozygous loss of a genomic region within the NF1 locus results in a dramatic drop of the signal intensity (Log R ration). Consequently, the signals for B allele frequencies are also altered.

(C) Sequence analysis of the NF1 H553R (1658A>G) missense mutation in a patient with a history of neurofibromatosis type I and a primary ganglioneuroma. Red arrows indicate the position of the mutant base in the transcript (c.DNA) and genomic DNA (g.DNA). The 1658A>G mutation was homozygous on the transcript level, whereas the mutation status of the genomic DNA was clearly heterozygous. A control genomic DNA is shown at the bottom.

Fig S5

SK-N-AS

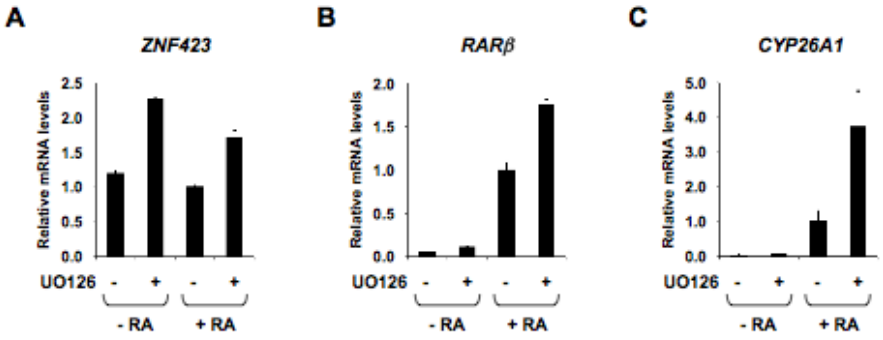
A
ZNF423
Relative mRNA levels
2.5
2.0
1.5
1.0
0.5
0.0
UO126 - + - +
- RA + RA
B
RARβ
Relative mRNA levels
2.0
1.5
1.0
0.5
0.0
UO126 - + - +
- RA + RA
C
CYP26A1
Relative mRNA levels
5.0
4.0
3.0
2.0
1.0
0.0
UO126 - + - +
- RA + RA

Figure S5. Induction of *ZNF423* by MEK inhibitor treatment and hyperactivation of *RARß* in the combination with RA in SK-N-AS cells, a neuroblastoma cell line with naturally occurring low NF1. Related to figure 7.

SK-N-AS cells were treated for 1 day with or without RA (1µM) and the MEK inhibitor U0126 (5µM). Relative expression levels of *ZNF423* (A) *RARß* (B) and *CYP26A1* (C), two bona fide RA target genes, were determined by qRT-PCR.

Table S1. The list of genes regulated by knockdown of NF1 in SH-SY5Y cells. Related to figure 4.

Global gene expression analysis in SH-SY5Y cells expressing both sh*NF1*#1 or sh*NF1*#2. 196 and 167 genes were greater than 2-fold up- or down-regulated, respectively in both *NF1* knockdown cell lines.

Table S2. Multivariate analysis of the AMC and Oberthuer cohorts. Related to figure 5.

Multivariate analysis of the AMC and Oberthuer cohort using *NF1* and *NF1/ZNF423* combined expression status and other clinically relevant parameters including *MYCN* amplification, LOH 1p, age and stage (see also Experimental Procedures). For the Oberthuer cohort only the *MYCN* status was public available. Expression of *NF1* predicted survival independently of *MYCN* amplification in both cohorts and patient age in the AMC cohort. CI denotes confidence intervals; the statistically significant parameters are shown in bold. All patients of the AMC cohort (n=88) were included in the entire analysis except the studies with LOH1p (n=82) due to the undetermined LOH 1p status in 6 patients. Multivariate analysis of the Oberthuer cohort is shown for the validation set (n=126) and the total cohort (n=251).

Supplemental Experimental Procedures

Reagents and Antibodies

All-trans retinoic acid (R2625) and MEK inhibitor U0126 (U120) were from Sigma. Antibodies against NF1 (SC-67), HSP90 (H-114), γ-Tubulin (H-183), p-ERK (E-4), ERK1 (C-16) and ERK2 (C-14) were from Santa Cruz Biotechnology; anti-ZNF423 (611407) was from BD Transduction laboratories. An additional antibody against NF1 was from Bethyl Laboratories (A300-140A). Antibodies against p-ERK (#9106), p-AKT Ser473 (#4051) and total AKT (#9272) were from Cell Signaling. A mixture of ERK1 and ERK2 antibodies was used for detection of total ERK.

Plasmids

All retroviral shRNA vectors were generated by ligating synthetic oligonucleotides (Invitrogen) against the target genes into in the pRetroSuper (pRS) retroviral vector as described (Brummelkamp et al., 2002). The RNAi target sequences were used for this study are as follows: sh*GFP*, 5'-GCTGACCCTGAAGTTCATC-3'; sh*NF1*#1, 5'-GTAGAATTGGCAGACTCCA-3'; sh*NF1*#2, 5'- GGAGAACTCCCTATAGCGA-3'; sh*NF1*#3, 5'-TGAAGAAACCAGTGAAGAA-3'; sh*KRAS*, 5'-GTTGGAGCTGGTGGCGTAG-3'.

The RARE-Luciferase reporter and pMSCV-*GFP*-PGK-*hZNF423-IRES2-PURO* (pMSCV-*ZNF423*) were as described previously (Huang et al., 2009). pQCXIP-*GFP* and pQCXIP-*NF1-GRD* were generated by cloning *GFP* and *NF1-GRD* into a gateway

compatible version of pQXCIP (Promega). The *NF1-GRD* entry vector (pENTR3C-*NF1-GRD*) was a kind gift of Dr. F. McCormick. Retroviral expression constructs (pBabe) for $KRAS^{G12V}$ (#12544), MEK-DD (#15268), $RALA^{Q75L}$ (#19719), $RALB^{Q72L}$ (#19721) and $PIK3CA^{H1047R}$ (#12524) were obtained from Addgene and sequence validated. The pBabe-$BRAF^{V600E}$ plasmid was a kind gift of Daniel Peeper. The cDNA encoding Myr-AKT was cloned into pBabe-puro and validated by sequencing.

Cell Culture and Viral Transduction

The human neuroblastoma cell lines are from the laboratory collections of Dr. R. Bernards and Dr. R. Versteeg and DSMZ (German Collection of Microorganisms and Cell Cultures). For all studies with retroviral infection presented, the subclones of each relevant line expressing the murine ecotropic receptor were generated. Cells were cultured in Dulbecco's modified Eagle's medium (DMEM) supplemented with 8% heat-inactivated fetal calf serum (FCS), penicillin and streptomycin. Retroviral transductions were performed using Phoenix cells as producers of viral supernatants as described (www.stanford.edu/group/nolan/retroviral_systems/phx.html). Infected cells were selected for successful retroviral integration using 1-2 μg/ml of puromycin. For the epistasis analysis in SH-SY5Y cells using sh*NF1* and sh*KRAS* (Figure 2G and 2H), cells were co-infected with viruses containing sh*NF1* and pRS in a ratio of 1 to 9 or co-infected with viruses containing sh*NF1* and sh*KRAS* in a ratio of 1 to 9. For the experiments that re-expression of ZNF423 reversed the RA resistance driven by *NF1* knockdown (Figure 4C and 4D), SH-SY5Y cells expressing MSCV control or MSCV-*ZNF423* were retro-virally infected with viruses containing pRS or sh*NF1* diluted with

pRS in ratio of 1 to 4.

Transfections and Reporter Assays

Transfections were carried out using calcium phosphate precipitation. RARE-luciferase reporter assays were performed in DMEM supplemented with charcoal-stripped FCS (HyClone, Logan, UT) essentially as described (Epping et al., 2007; Huang et al., 2009).

Quantitative RT–PCR (qRT-PCR)

QRT-PCR assays were carried out to measure mRNA levels of genes using 7500 Fast Real-Time PCR System (Applied Biosystems) as described (Kortlever et al., 2006). Relative mRNA levels of each gene shown were normalized to the expression of the house keeping gene *GAPDH*. The sequences of the primers for assays using SYBR® Green master mix (Roche) are as follows: *NF1*_QPCR_Forward, 5'-TGTCAGTGCATAACCTCTTGC-3'; *NF1*_QPCR_Reverse, 5'-AGTGCCATCACTCTTTTCTGAAG; *NF1-GRD*_QPCR_Forward, 5'-GGGCAGTATCTTTCCAGCAA-3'; *NF1-GRD*_QPCR_Reverse, 5'-GAGGACCCAGGTATGCAAGA-3'; *ZNF423*_QPCR_Forward, 5'-TGACGACCCACAACTCTCCT-3'; *ZNF423*_QPCR_Reverse, 5'-GAACTGGCAAGGGTATGGCAG-3'; *KRAS*_QPCR_Forward, 5'-GGACTGGGGAGGGCTTTCT-3'; *KRAS*_QPCR_Reverse, 5'-GCCTGTTTTGTGTCTACTGTTCT-3'; *RARb*_QPCR_Forward, 5'-TGAGTCCTGGGCAAATCCTG-3'; *RARb*_QPCR_Reverse, 5'-CGGTTTGGGTCAATCCACTGA-3'; *CRABP2*_QPCR_Forward, 5'-

TCGGAAAACTTCGAGGAATTGC-3’; *CRABP2*_QPCR_Reverse, 5’-CCTGTTTGATCTCCACTGCTG-3’; *TGM2*_QPCR_Forward, 5’-CAACCTGGAGCCTTTCTCTG-3’; *TGM2*_QPCR_Reverse, 5’-GCACCTTGATGAGGTTGGAC-3’; *CYP26A1*_QPCR_Forward, 5’-TCTGATCACTTACCTGGGGC-3’; *CYP26A1*_QPCR_Reverse, 5’-TTCCAAAATTTCCATGTCCAA-3’; *RET*_QPCR_Forward, 5’-GGCATCAACGTCCAGTACAAG; *RET*_QPCR_Reverse, 5’-TGAGGTGACCACCCCTAGC-3’.

Microarray Analysis - AMC and CHLA patient cohorts

The *NF1* and *ZNF423* expression data of the two independent cohorts (AMC and CHLA) were both obtained using Affymetrix platform (U133 Plus 2.0 or U133A) as described (Asgharzadeh et al., 2006; Huang et al., 2009). The optimal cut-off value (192.8) for *NF1* expression in the AMC cohort was determined using kaplan scanning as described (Huang et al., 2009). In short, the neuroblastoma patients were sorted based on expression of *NF1* (212678_at) and subsequently divided into two groups based on the expression value of each patient (with a minimum group size of 20 patients). For each group separation (higher or lower than the current *NF1* expression), the log-rank significance was calculated. The best p-value out of the sequence was then used to represent the final gene expression cutoff value for *NF1*. In a leave-one-out cross-validation scheme, the same cutoff was chosen 86 out of 88 times and prediction of the left out sample was significant ($p<0.021$ fisher exact). For the validation study, *NF1* expression of the second independent cohort (CHLA) was first normalized as described

(Huang et al., 2009). The *NF1* cut-off value (192.8) of the AMC cohort in U133 Plus 2.0 setting was translated into 104.8 in U133A setting for CHLA. This translated *NF1* cut-off value was then used to classify the patients from the second independent cohort for the progression-free survival analysis.

For the progression-free survival analysis using the combined expression status of *NF1* and *ZNF423*, The *NF1* cut-off value was the same as above and *ZNF423* cut-off value was as described previously (Huang et al., 2009).

For the multivariate analysis, Cox regression calculations on progression-free survival were performed in SPSS version 15.0. For these calculations single covariates (*NF1*, *MYCN*, LOH1p, stage, age) as well as double covariates in a non-sequential model (*MYCN*, LOH1p, stage, age) in combination with the *NF1* cut-off were used. The variable stage consisted two groups based on INSS: 1) ST1, 2, 3 and 4S; 2) ST4. The variable age (of diagnosis) consisted two groups: 1) <=18 months; 2) > 18 months. Hazard ratio's, p-values and 95% confidence intervals were part of the SPSS output.

Microarray Analysis – Oberthuer patient cohort

The normalized Oberthuer dataset was downloaded from ArrayExpress (E-TABM-38). The provided outdated annotation was updated using the probe sequences (obtained from A-MEXP-255) with BLAT against a recent reference sequence database (2010-jan-25). We have used probe A-MEXP-255.3956 to represent the ZNF423 gene and A-MEXP-255.8758 to represent NF1. The dataset was randomly divided into 2 groups of equal size (n=125 / n=126). One group (n=125) was subsequently used to scan for a cutoff, while the second group (n=126) was used as an independent cohort for validation. The Kaplan

scanning method and multivariate analyses are as described for the AMC and CHLA cohorts.

Microarray Analysis – SH-SY5Y

The microarray analysis of SH-SY5Y neuroblastoma cells expressing pRS control or sh*NF1*#1 or sh*NF1*#2 was performed using the same Affymetrix platform as described above.

***NF1* Mutational Analysis**

The entire *NF1* coding region was amplified in five overlapping RT-PCR fragments and used as the template for direct sequencing as described (Messiaen et al., 2000). Copy number analysis by multiplex ligation-dependent probe amplification was performed as described (Wimmer et al., 2006). The nomenclature of the mutations is based on *NF1* mRNA sequence NM_000267.1, with 1 being the first nucleotide of the ATG start codon. The *NF1* exons are named according to the most widely used nomenclature adapted by the researchers and diagnostic labs, which does not use strictly consecutive numbers.

Deletion analysis of neuroblastoma cell lines

DNA was extracted according to standard methods from tumor samples acquired at diagnosis and neuroblastoma cell lines. DNA was quantified with NanoDrop, and the quality was verified by 260/280 and 260/230 abs. SNP microarray BeadChips were processed according to the manufacturer's recommendations with the Infinium II assay on Human370 / 660-quad arrays containing > 370.000/ > 660 000 markers and run on the Illumina® Beadstation (Swegene Centre for Integrative Biology, Lund University -

SCIBLU, Sweden) according to the manufacturer's recommendations. Raw data were processed using Illumina's GenomeStudio software suite (genotyping module V1.0), producing report files containing normalized intensity data and SNP genotypes and copy number. Subsequently, $\log_2$ ratio and B-allele frequency (BAF) data were imported into Nexus Copy Number Software (V4.1, BioDiscovery) and our own R2 software for visualization and analysis. All aberrations were visually checked in GenomeStudio. The following 20 neuroblastoma cell lines analysis were used for the SNP analysis: SK-N-F1, Gi-MEN, SK-N-AS, SJ-NB12, IMR32, SJ-NB8, SJ-NB10, NMB, SH-SY5Y, NGP, KCNR, N206, TR14, SK-N-BE, SJ-NB1, LAN5, LAN1, AMC106, UHGNP and SJ-NB6.

Supplemental references

Brummelkamp, T.R., Bernards, R., and Agami, R. (2002). A system for stable expression of short interfering RNAs in mammalian cells. Science *296*, 550-553.

Epping, M.T., Wang, L., Plumb, J.A., Lieb, M., Gronemeyer, H., Brown, R., and Bernards, R. (2007). A functional genetic screen identifies retinoic acid signaling as a target of histone deacetylase inhibitors. Proc Natl Acad Sci U S A *104*, 17777-17782.

Kortlever, R.M., Higgins, P.J., and Bernards, R. (2006). Plasminogen activator inhibitor-1 is a critical downstream target of p53 in the induction of replicative senescence. Nature cell biology *8*, 877-884.